

## A Numerical Study of Forced Convection Heat Transfer for Staggered Tube Banks in Cross-Flow

T. A. Tahseen<sup>1</sup>, M. Ishak<sup>1,2</sup> and M. M. Rahman<sup>1,2</sup>

<sup>1</sup>Faculty of Mechanical Engineering, University Malaysia Pahang  
26600 Pekan, Pahang, Malaysia

Phone : +609-424-2246 ; Fax : +609-424-2202

Email: tahseen444@gmail.com; mahadzir@ump.edu.my;  
mustafizur@ump.edu.my

<sup>2</sup>Automotive Engineering Centre, Universiti Malaysia Pahang,  
26600 Pekan, Pahang, Malaysia.

**Abstract:** This paper presents the numerical study on the two-dimensional forced convection heat transfer for staggered tube banks in cross flow under incompressible, steady-state conditions. This system is solved on the body fitted coordinates (BFC) using the finite difference method (FDM) for the flow over a bundle of cylindrical tubes. The constant heat flux is imposed on the surface of the tubes as the thermal boundary condition. The type of the arrangement is considered a staggered of tubes. The longitudinal pitch to tube diameter ratios ( $S_T/D$ ) of 1.25, 1.5 and 2 are also considered. Reynolds numbers are varied from 25 to 250 and Prandtl number is taken as 0.71. Velocity field vectors and temperature contours, local and average Nusselt numbers were analysed in this paper. It can be seen that the predicted results are good agreements with previous experimental and numerical results. The obtained results show that the heat transfer rate increases with decreases of the step to the longitudinal tube diameter. The local heat transfer strongly depends on the Reynolds number. It tends to obtain the highest values at the surface opposite to the direction of flow. The heat transfer rate is insignificant in the areas of recycling.

**Keywords:** Forced convection, cylindrical tube, staggered arrangement, body fitted coordinates, finite different method.

### 1. Introduction

The flow of fluids and heat transfer in tube banks represents an idealization of many industrially important processes. Tube bundles are widely employed in cross-flow heat exchangers, the design is still based on empirical correlations of heat transfer and pressure drop. Heat exchangers with tube banks in cross-flow are of great practical interest in many thermal and chemical engineering processes (Incropera and Dewitt, 1996; Buyruk, 2002; Mandhani et al. 2002; Liang and Papadakis, 2007; Kaptan et al., 2008). A two dimensions numerical study pressure drop, heat transfer and incompressible laminar flow for staggered tube arrays in cross-flow (Yuan et al., 1998; Rahmani et al., 2005; Khan et al., 2006; Marchi and Hobmeir, 2007). The low Reynolds number and Prandtl number equal to 0.71 are considered in general (Chang et al., 1989; Wang and Georgiadis, 1996). An experimental study was carried out to investigate heat transfer and flow characteristics from one tube within a staggered tube bundle and within a row of similar tubes. Variation of a local Nusselt number and local pressure coefficients were shown with different blockages and Reynolds numbers (Buyruk et al., 1998; Buyruk, 1999; Matos et al., 2001, 2004). The experimental and numerical study pressure drop and heat transfer

through bundles of parallel cylinders. The numerical results cover the range  $1 \leq Re_D \leq 30$ ,  $0.72 \leq Pr \leq 100$ ,  $0.6 \leq \Phi \leq 0.95$  and  $0^\circ \leq \beta \leq 60^\circ$ , where  $\Phi$  is the porosity of the bundle as a saturated porous medium, and  $\beta$  is the angle between the cylinder centreline. The experimental measurements in the range of  $1 \leq Re_D \leq 30$ ,  $0.84 \leq \Phi \leq 0.92$  and  $0^\circ \leq \beta \leq 60^\circ$ . The results show that the significant errors may occur if the available large- $Re_D$  information is extrapolated to the domain covered by this study (Fowler and Bejan, 1994). This is an experimental, numerical and analytical study of the optimal spacing between cylinders in cross-flow forced convection. The experimental  $Re_D$  range of 50- 4000 and the second part, similar results are developed based on numerical simulations for  $Pr = 0.72$  and  $40 \leq Re_D \leq 200$ . The experimental and numerical results for optimal spacing and maximum thermal conductance are explained and correlated analytically by intersecting the small-spacing and large- spacing asymptotes of the thermal conductance function (Stanescu et al., 1996). A calculation procedure for two-dimensional elliptic flow is applied to predict the pressure drop and heat transfer characteristics of laminar and turbulent flow of air across tube banks. The theoretical results of the present model are compared with previously published experimental data (Wilson and Bassiouny, 2000). Cross-flow over tube banks are commonly encountered in practice in heat transfer equipments. The average Nusselt number increases more than 30% and 65% on the second and third tubes, respectively, in comparison with that of the first tube (Yoo et al., 2007). The objective of this study is to numerical study of the two-dimension laminar incompressible flow and heat transfer over a staggered circular tube bank. The local and average heat transfer characteristics for staggered tube banks are investigated in the present study.

## 2. Methodology

The treated problem is a two-dimensional of a staggered tube bank with the diameter of tube 15mm and the  $S_L=15$ mm. The equations governing the conservation of continuity, momentum, and energy equation. Assuming constant thermophysical properties of the fluid, with two-dimensional expressions in Cartesian vector notation for steady-state incompressible flow. The physical system considered in the present study is displayed in 'figure 1', are (Bejan, 1995):

$$\text{Continuity:} \quad \frac{\partial U}{\partial X} + \frac{\partial V}{\partial Y} = 0 \quad (1)$$

Momentum (Navier-Stokes):

$$\left. \begin{aligned} \text{X-direction (u momentum)} \quad U \frac{\partial V}{\partial X} + V \frac{\partial V}{\partial Y} &= -\frac{\partial P}{\partial X} + \frac{1}{Re_D} \left[ \frac{\partial^2 U}{\partial X^2} + \frac{\partial^2 U}{\partial Y^2} \right] \\ \text{Y-direction (v momentum)} \quad U \frac{\partial V}{\partial X} + V \frac{\partial V}{\partial Y} &= -\frac{\partial P}{\partial Y} + \frac{1}{Re_D} \left[ \frac{\partial^2 V}{\partial X^2} + \frac{\partial^2 V}{\partial Y^2} \right] \end{aligned} \right\} \quad (2)$$

$$\text{Energy:} \quad U \frac{\partial \theta}{\partial X} + V \frac{\partial \theta}{\partial Y} = \frac{1}{Pr Re_D} \left[ \frac{\partial^2 \theta}{\partial X^2} + \frac{\partial^2 \theta}{\partial Y^2} \right] \quad (3)$$

The dimensionless variables have been defined based on appropriate physical scales as Eq. (4):

$$(X, Y) = \frac{(x, y)}{D}, P = \frac{p}{\rho U_\infty^2}, (U, V) = \frac{(u, v)}{U_\infty}, \theta = \frac{T - T_\infty}{T_w - T_\infty}, Re_D = \frac{U_\infty D}{\nu}, Pr = \frac{C_p \mu}{k} \quad (4)$$

The schematic of staggered tube banks and computational domain is shown in figure 1. Boundary conditions are as follows:

$$\begin{aligned} \text{(I)} \quad U &= 1, \quad \frac{\partial V}{\partial X} = 0, \quad \theta = 0 \\ \text{(B)} \quad \frac{\partial U}{\partial Y} &= 0, \quad V = 0, \quad \frac{\partial \theta}{\partial Y} = 0 \\ \text{(A)} \quad U &= V = 0, \quad \theta = 1 \\ \text{(E)} \quad \frac{\partial U}{\partial X} &= \frac{\partial V}{\partial X} = 0, \quad \frac{\partial \theta}{\partial X} = 0 \end{aligned}$$

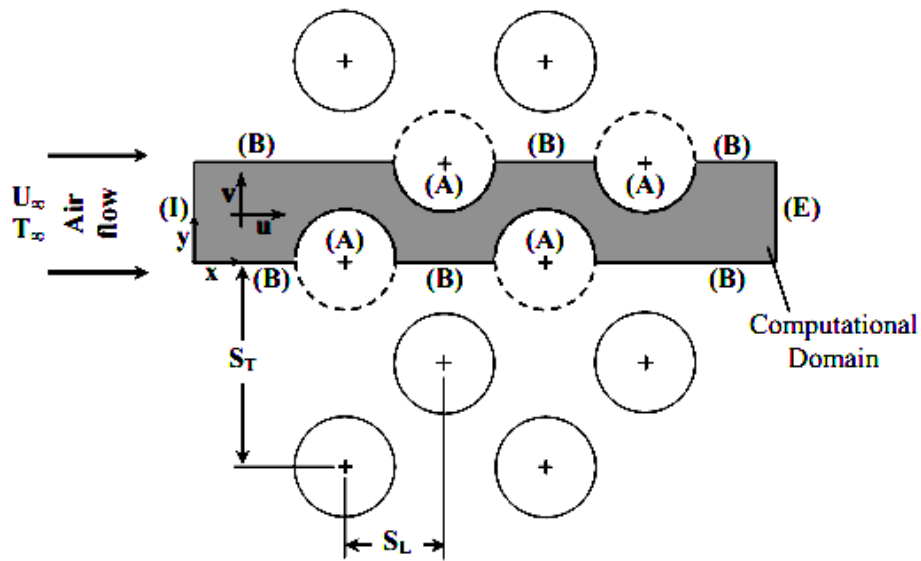


**Figure 1.** Schematic of staggered tube banks and computational domain

The heat transfer coefficient ( $h$ ) can be expressed in the dimensionless form by the local and average Nusselt numbers  $Nu$  and  $\bar{Nu}$ , which is defined as Eq. (5) and Eq. (6) respectively (Chen and Wung, 1989):

$$Nu = \frac{hD}{k} = \left. \frac{\partial \phi}{\partial n} \right|_{\phi} \quad (5)$$

$$\bar{Nu} = \frac{\bar{h}D}{k} = \left( \int_{\phi} Nuds \right) / \left( \int_{\phi} ds \right) \quad (6)$$

The set of conservation (Eq. 2 and Eq. 4) can be written in general form in Cartesian coordinates as Eq. (7):

$$\frac{\partial(U\phi)}{\partial X} + \frac{\partial(V\phi)}{\partial Y} = \frac{\partial}{\partial X} \left( \Gamma \frac{\partial \phi}{\partial X} \right) + \frac{\partial}{\partial Y} \left( \Gamma \frac{\partial \phi}{\partial Y} \right) + S_{\phi} \quad (7)$$

The continuity equation, Eq. (1) has no diffusion and source terms. It will be used to derive an equation for the pressure correction. The grid generation scheme based on elliptic partial differential equations is used in the present study to generate the curvilinear coordinates. Eq. (7) can be transformed from the physical domain to the computational domain according to the following transformation  $\zeta = \zeta(x, y), \eta = \eta(x, y)$  (Thompson et al. 1985). The final form of the transformed equation can be written as Eq. (8):

$$\frac{\partial}{\partial \zeta} (\phi G_1) + \frac{\partial}{\partial \eta} (\phi G_2) = \frac{\partial}{\partial \zeta} \left( \frac{\Gamma}{J} \left( \alpha \frac{\partial \phi}{\partial \zeta} - \gamma \frac{\partial \phi}{\partial \eta} \right) \right) + \frac{\partial}{\partial \eta} \left( \frac{\Gamma}{J} \left( \beta \frac{\partial \phi}{\partial \eta} - \gamma \frac{\partial \phi}{\partial \zeta} \right) \right) + JS_{\phi} \quad (8)$$

Where:

$$\left. \begin{aligned} G_1 &= U \frac{\partial Y}{\partial \eta} - V \frac{\partial X}{\partial \eta}, & G_2 &= V \frac{\partial X}{\partial \zeta} - U \frac{\partial Y}{\partial \zeta}, & J &= \left( \frac{\partial X}{\partial \zeta} \frac{\partial Y}{\partial \eta} - \frac{\partial Y}{\partial \zeta} \frac{\partial X}{\partial \eta} \right) \\ \alpha &= \left( \frac{\partial x}{\partial \eta} \right)^2 + \left( \frac{\partial y}{\partial \eta} \right)^2, & \gamma &= \left( \frac{\partial x}{\partial \zeta} \frac{\partial x}{\partial \eta} \right) + \left( \frac{\partial y}{\partial \zeta} \frac{\partial y}{\partial \eta} \right), & \beta &= \left( \frac{\partial x}{\partial \zeta} \right)^2 + \left( \frac{\partial y}{\partial \zeta} \right)^2 \end{aligned} \right\} \quad (9)$$

Eq., (8) was solved numerically using a control volume-based finite difference method. The solved by the marching type procedure involving a series of two dimensional elliptic problem in the cross-stream plane. The marching step size is  $1 \times 10^{-4}$  along the axial distance. At each marching step, the strong coupling of pressure and velocity in the cross section was calculated by the SIMPLER-algorithm on a collocated non-orthogonal grid. It is used to adjust the velocity field to satisfy the conservation of mass (Patankar, 1980). For the computational calculations, a computer code was prepared in FORTRAN-90. In the numerical calculation, a  $146 \times 21$  grid arrangements are found to be sufficient for grid independent solution and then the 2D-algebraic grid is generated.

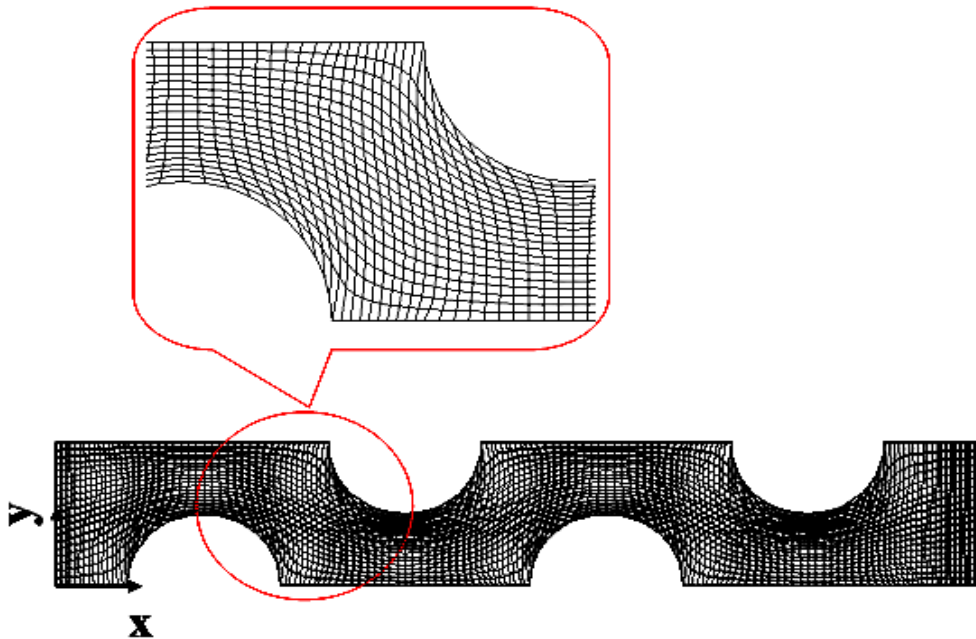


**Figure 2.** Schematic of grid systems generated by body-fitted coordinates.

### 3. Validation

The numerical model was validated with some of previous published benchmark problems. The fluid flow and heat transfer over a row of in a staggered circular tube subjected to constant wall temperature and constant heat flux were predicted. The Nusselt number for the fully developed region between two tubes subjected to constant wall temperature using by previous literatures. 'Figure 3' shows comparison between the present study with previous literatures (( Kaptan et al., 2008; Buyruk, 2002) for local Nusselt number with  $Re = 120$ ,  $Pr = 0.71$  and  $S_T/D = 2.0$ . It can be seen that an excellent agreement is achieved between the present results and the numerical results of Kaptan et al. (2008) and Buyruk (2002), for the local Nusselt number distribution circumference of the first tube.

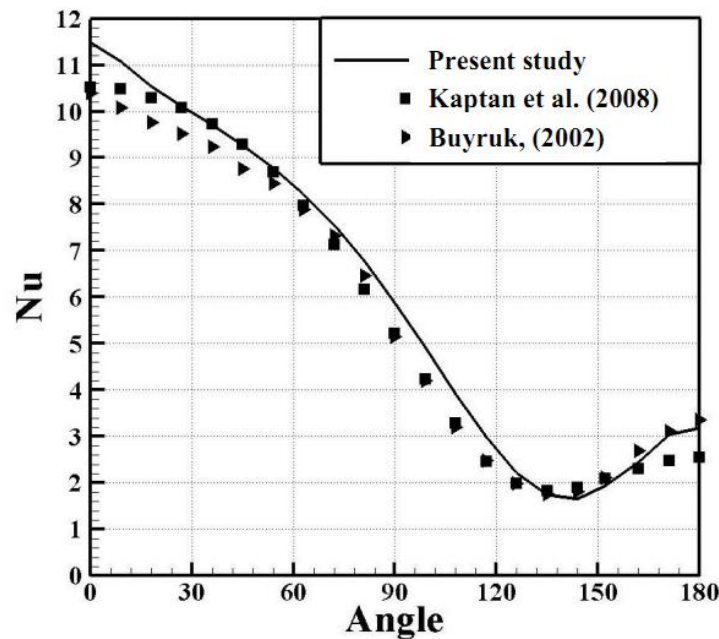
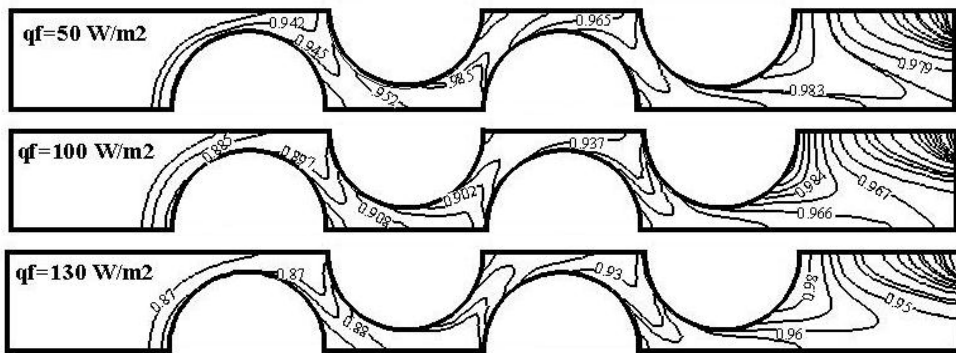


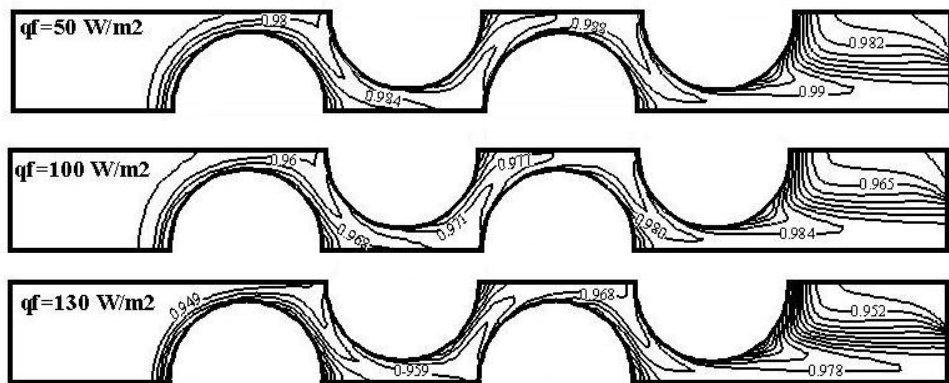
**Figure 3.** Comparison between the present study with previous literatures (Kaptan et al., 2008; Buyruk, 2002) for local Nusselt number with  $Re = 120$ ,  $Pr = 0.71$  and  $S_T/D = 2.0$

#### 4. Results and Discussion

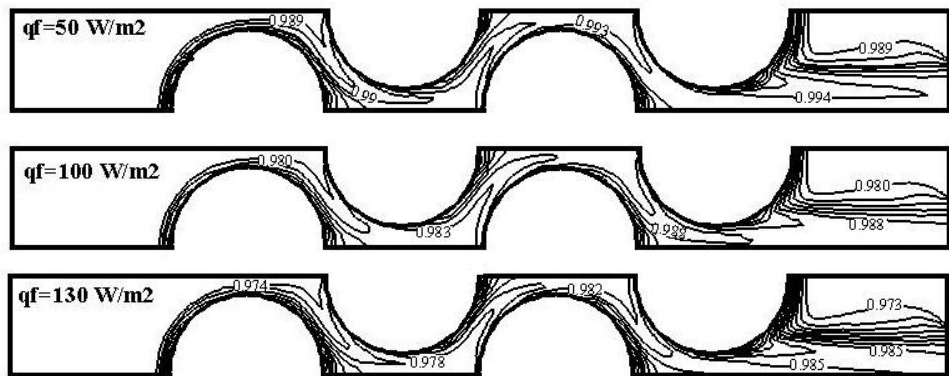
The numerical solutions of convective heat transfer of a cross tube bundle staggered. The transverse pitch ( $S_T$ ) have been a varied for 1.25, 1.5 and 2.0. The range of Reynolds numbers are 25 to 250. Heat flux ( $q_f$ ) in the surface tubes also varies from 50, 100 and 130 W/m<sup>2</sup>. The normalized temperature lines (isotherms) are presented in the temperature distributions within a range of 0 to 1. 'Figure 4-6' show the temperature distribution for various longitudinal pitch to tube diameter ratios  $S_T/D$ , Reynolds numbers as well as heat flux in tube surface. A general view of the plots a low fluid temperature at the inlet to higher fluid temperature as it reaches the hot tube surface because of the wavy motion of the through a stream as the isolation of the separation zone behind the cylinder. The temperature contours are packed along the upstream facing surface and diffused into the downstream. In the separation zone, the thermal layer is relatively thick, particularly near the separation point. As the Reynolds number increases, the lower value isotherms penetrate deeper, which means the colder fluid is getting closer to the hot surface. As a result of this behavior, the heat transfer is increased.



(a)

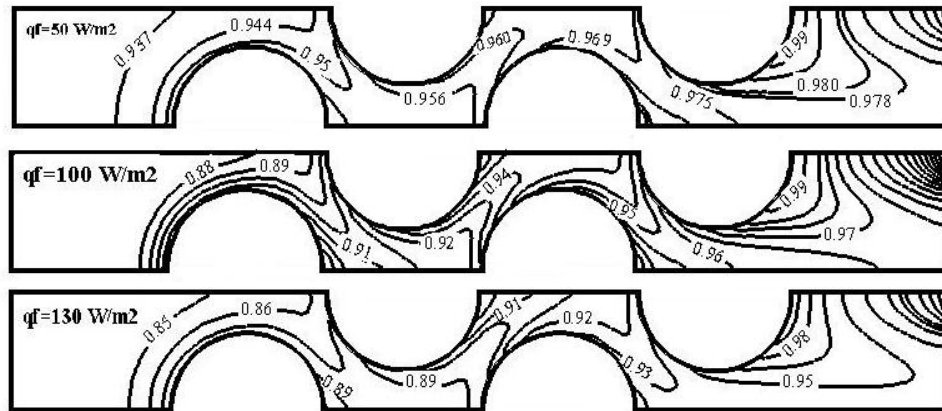


(b)

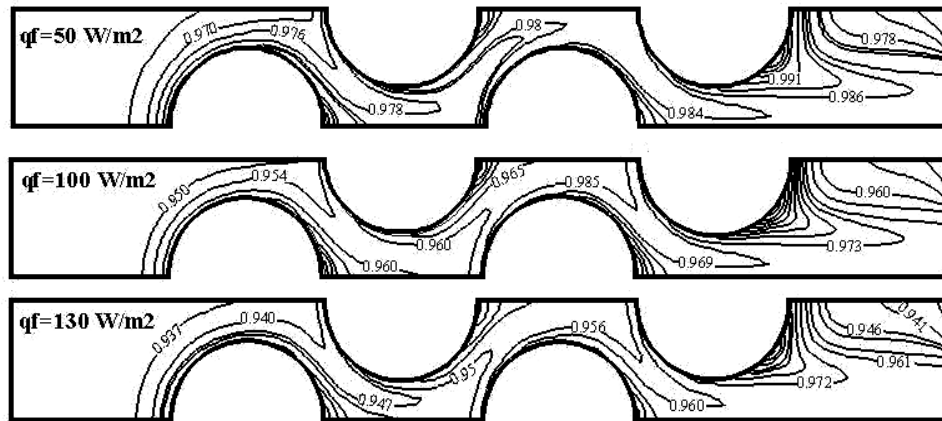


(c)

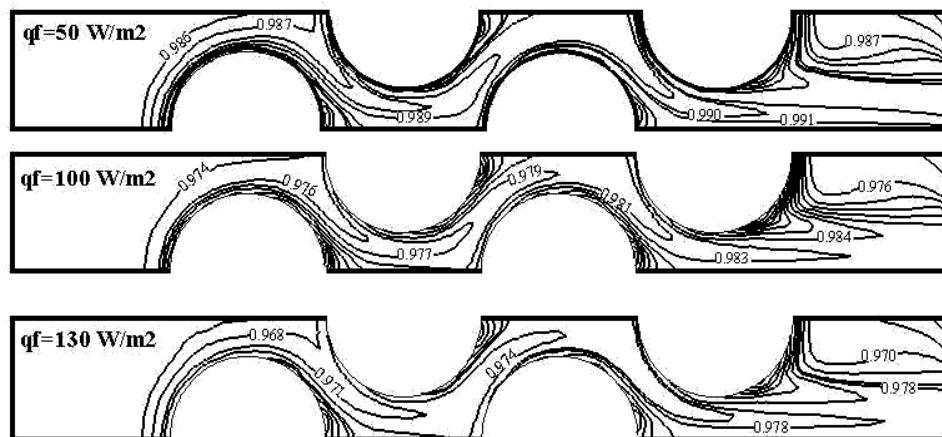
**Figure 4.** Temperature distribution at  $S_T/D=1.25$  and Reynold's number of (a) 25, (b) 100 and (c) 250



(a)

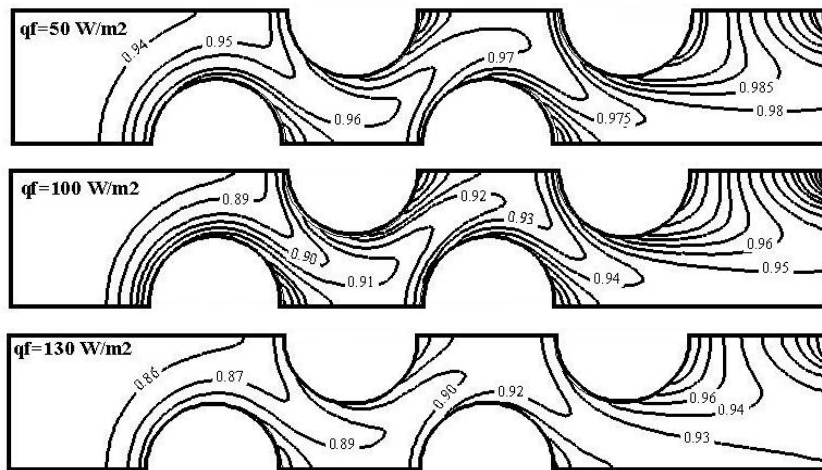


(b)

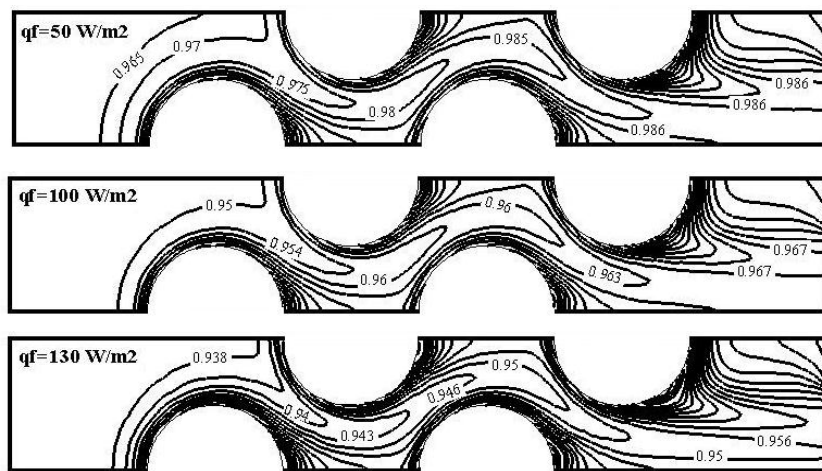


(c)

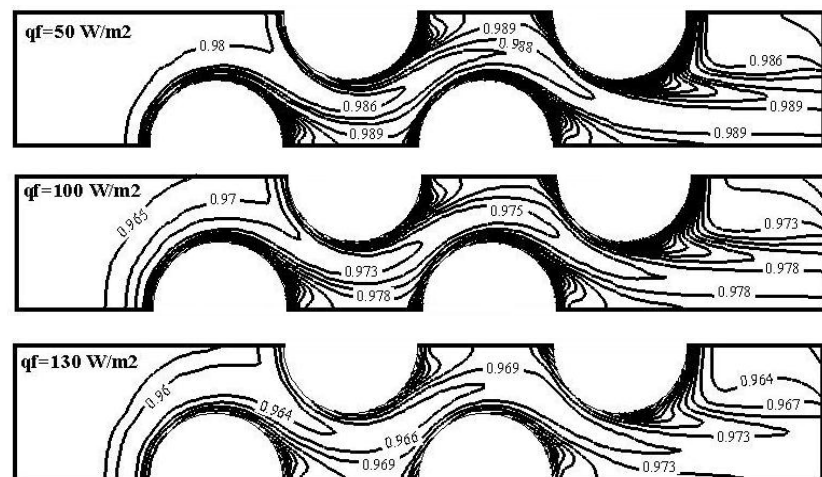
**Figure 5.** Temperature distribution at  $S_T/D=1.50$  and Reynold's number of (a) 25, (b) 100 and (c) 250



(a)



(b)

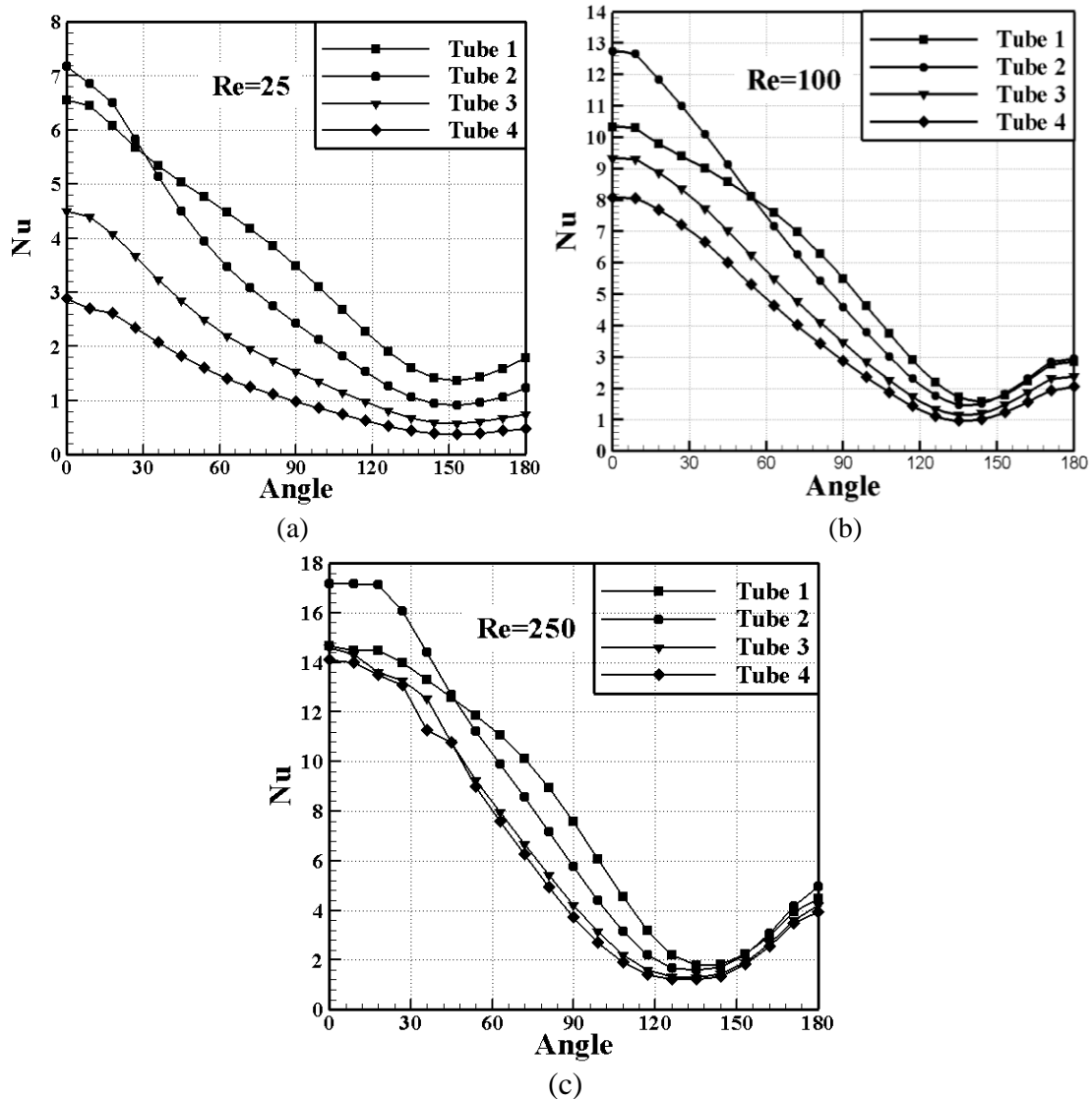


(c)

**Figure 6.** Temperature distribution at  $S_T/D=2.0$  and Reynold's number for (a) 25, (b) 100 and (c) 250

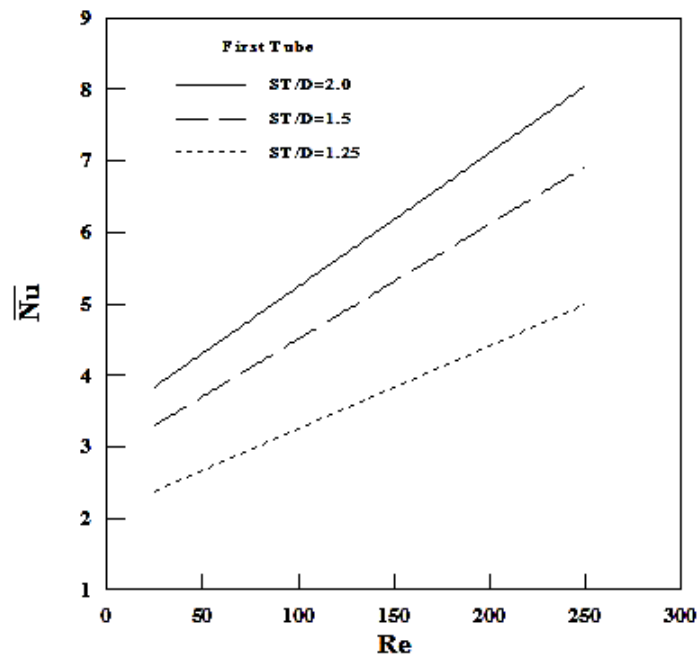


Figure 7 presents the relationship between of the local Nusselt number and the angle of a round tube surface for various Reynold's number and the location of a tube. A laminar boundary layer develops from the front stagnation point for a cylinder in cross-flow and grows in thickness around the cylinder. The maximum heat transfer rate is located close to the front stagnation point and the local Nusselt number decrease with the angle. The position of the minimum local Nusselt number is not fixed around 153 deg at  $Re = 25$ , 140 deg at  $Re = 100$  and 135 deg at  $Re = 250$ . It is noted that the minimum values of local Nusselt number a rein the third and fourth tube.



**Figure 7.** Local Nusselt number distribution of the location of tube with  $S_T/D=2.0$  for Reynold's number of (a) 25, (b) 100 and (c) 250

Figure 8 presents the effect of mean Nusselt number with Reynold's number for the first tube at  $Pr = 0.71$ . It can be seen that the mean Nusselt number is increased with the increase of Reynold's number as well as the longitudinal pitch to tube diameter ratio  $S_T/D$ . The variation of Nusselt number is more significant at higher Reynold's number.



**Figure 8.** Variation of mean Nusselt number with  $Re$  for the first tube at  $Pr = 0.71$

## 5. Conclusions

The flow and heat transfer tubes in the regulation of cross-flow is of great importance in many engineering applications. The two-dimensional steady-state and incompressible laminar flow for staggered tube arrays in cross-flow is investigated numerically. A finite difference method is numerically used to solve the governing Navier-Stokes and energy equations. The results show that the behavior of flow and heat transfer of the first tube is similar to the behavior of flow and heat transfer of a single tube. The local Nusselt number is increases by increases the longitudinal pitch to tube diameter ratios and decreasing the angle of the surface tube. The average Nu number increases by increases Reynolds number or by increases the longitudinal pitch to tube diameter ratios. The form of temperature distribution is affected by Reynolds number.

## Acknowledgements

The authors would like to thank Universiti Malaysia Pahang for providing laboratory facilities and financial support under Doctoral Grant scheme.

## References

- [1] Bejan A 1995 *Convection Heat Transfer* New York: John Wiley.
- [2] Buyruk E 1999 Heat transfer and flow structures around circular cylinders in cross-flow *Tr. J. of Engineering and Environmental Science* **23** 299-315.
- [3] Buyruk E 2002 Numerical study of heat transfer characteristics on tandem cylinders inline and staggered tube banks in cross-flow of air *International Communications in Heat and Mass Transfer* **29** 355-366.
- [4] Buyruk E, Johnson M W, Owen I 1998 Numerical and experimental study of flow and heat transfer around a tube in cross-flow at low Reynolds number *International Journal of Heat and Fluid Flow* **19** 223-232.
- [5] Chang Y, Beris A N, Michaelides E E 1989 A numerical study of heat and momentum transfer for flexible tube bundles in cross flow *International Journal of Heat and Mass Transfer* **32** 2027-2036.

- [6] Chen C J, Wung T S 1989 Finite analytic solution of convective heat transfer for tube arrays in cross-flow: Part II-Heat transfer analysis *Journal of Heat Transfer* **111** 641-648.
- [7] Fowler A J, Bejan A 1994 Forced convection in banks of inclined cylinders at low Reynolds numbers *International Journal of Heat and Fluid Flow* **15** 90-99.
- [8] Incropera F P, Dewitt D P 1996 *Fundamentals of heat and mass transfer* New York: John Wiley.
- [9] Kaptan Y, Buyruk E, Eceder A 2008 Numerical investigation of fouling on cross-flow heat exchanger tubes with conjugated heat transfer approach. *International Communications in Heat and Mass Transfer* **35** 1153-1158.
- [10] Khan W A, Culham J R, Yovanovich M M 2006 Convection heat transfer from tube banks in cross-flow: analytical approach *International Journal of Heat and Mass Transfer* **49** 4831-4838.
- [11] Liang C, Papadakis G 2007 Large eddy simulation of cross-flow through a staggered tube bundle at subcritical Reynolds number *Journal of Fluids and Structures* **23** 1215-1230.
- [12] Mandhani V K, Chhabra R P, Eswaran V 2002 Forced convection heat transfer in tube banks in cross-flow *Chemical Engineering Science* **57** 379-391.
- [13] Marchi C H, Hobmeir M A 2007 Numerical solution of staggered circular tubes in two-dimensional laminar forced convection *J. of the Braz. Soc. of Mech. Sci. & Eng.* **XXIX** 42-48.
- [14] Matos R S, Vargas J V C, Laursen T A, Bejan A 2004 Optimally staggered finned circular and elliptic tubes in forced convection *International Journal of Heat and Mass Transfer* **47** 1347-1359.
- [15] Matos R S, Vargas J V C, Laursen T A, Saboya F E M 2001 Optimization study and heat transfer comparison of staggered circular and elliptic tubes in forced convection *International Journal of Heat and Mass Transfer* **44** 3953-3961.
- [16] Patankar S V 1980 *Numerical heat transfer and fluid flow* Hemisphere, Washington, DC.
- [17] Rahmani R, Mirzaee I, Shirvani H 2005 Computation of a laminar flow and heat transfer of air for staggered tube arrays in cross-flow *Iranian Journal of Mechanical Engineering* **6** 19-33.
- [18] Stanescu G, Fowler A J, Bejan A 1996 The optimal spacing of cylinders in free-stream cross-flow forced convection *International Journal of Heat and Mass Transfer* **39** 311-317.
- [19] Thompson J R, Warsi Z U A, Martin C W 1985 *Numerical grid generation, foundations and applications* North-Holland, New York.
- [20] Wang M, Georgiadis J G 1996 Conjugate forced convection in cross-flow over a cylinder array with volumetric heating *International Journal of Heat and Mass Transfer* **39** 1351-1361.
- [21] Wilson A S, Bassiouny M K 2000 Modeling of heat transfer for flow a cross tube banks *Chemical Engineering and Processing* **39** 1-14.
- [22] Yoo S Y, Kwonb H K, Kim J H 2007 A study on heat transfer characteristics for staggered tube banks in cross-flow *Journal of Mechanical Science and Technology* **21** 505-512.
- [23] Yuan Z X, Tao W Q, Wang Q W 1998 Numerical prediction for laminar forced convection heat transfer in parallel-plate channels with stream wise-periodic rod disturbances *Int. J. Numer. Meth. Fluids* **28** 1371-1387.

## Nomenclatures

$C_p$	Specific heat [ $J.Kg^{-1} K^{-1}$ ]	$J$	Jacobian of the transformation
$D$	Diameter of tube [m]	$Nu, \overline{Nu}$	Local and average Nusselt number
$G_1, G_2$	Contravariant velocity components	$p$	Pressure [ $N.m^{-2}$ ]
$h, \overline{h}$	local and average convection heat transfer coefficient [ $W.m^{-2}K^{-1}$ ]	$P$	Dimensionless pressure
$k$	Thermal conductivity of the fluid [ $W.m^{-1}K^{-1}$ ]	$Pr$	Prandtl number
$q_f$	Heat flux [ $W.m^{-2}$ ]	$\theta$	Dimensionless temperature
$Re_D$	Reynolds number based on tube diameter	$\mu$	Dynamic viscosity [ $N.s.m^{-2}$ ]
$T$	Temperature [ $^{\circ}C$ ]	$\nu$	Kinematic viscosity [ $m^2.s$ ]
$S$	Source term	$\rho$	Density [ $kg.m^{-3}$ ]
$S_L$	Longitudinal distance between two consecutive tubes [m]	$\zeta, \eta$	Curvilinear coordinates
$S_T$	Transverse distance between two consecutive tubes [m]	$\phi$	General dependent variable
$u, v$	Velocity components [ $m.s^{-1}$ ]	$\alpha, \beta, \gamma$	The coefficients of transformation
$U, V$	Dimensionless velocity components	$\Phi$	Boundary contour
$x, y$	Cartesian coordinates [m]	<b>Subscripts</b>	
$X, Y$	Dimensionless Cartesian coordinates	$\infty$	Free stream
<b>Greek symbols</b>		$s$	The infinitesimal distance on the contour
$\alpha$	Thermal diffusivity [ $m^2.s^{-1}$ ]	$w$	Wall of tube
$\Gamma$	Diffusion coefficient		